Available online at www.sciencedirect.com

ScienceDirect

Polymer 47 (2006) 6551–6559

polymer

www.elsevier.com/locate/polymer

Synthesis and properties of polyacetylenes carrying *N*-phenylcarbazole and triphenylamine moieties

Jinqing Qu, Ritsuya Kawasaki, Masashi Shiotsuki, Fumio Sanda*, Toshio Masuda*

Department of Polymer Chemistry, Graduate School of Engineering, Kyoto University, Katsura Campus, Kyoto 615-8510, Japan

Received 22 May 2006; received in revised form 27 June 2006; accepted 22 July 2006

Abstract

Novel acetylene monomers containing *N*-phenyl-substituted carbazole (Cz) and triphenylamine (TPA) groups, namely, 3-ethynyl-9-phenylcarbazole (**1**) and *p*-(*N*,*N*-diphenylamino)phenylacetylene (**2**) were synthesized, and polymerized with several Rh-, W-, and Mo-based catalysts. Poly(**1**) and poly(**2**) with high number-average molecular weights (15 500–974 000) were obtained in good yields (77–97%), when $[(nbd)RhCl]_2$–Et_3N (nbd = norbornadiene) was used as a catalyst. The polymers exhibited UV–vis absorption peaks derived from the Cz and TPA moieties at 250–350 nm and polyacetylene backbone above 350 nm. The UV–vis absorption band edge wavelengths of the polymers were longer than those of the corresponding monomers. Poly(**2**) exhibited a UV–vis absorption peak at a longer wavelength than poly(**1**) did, which indicates that poly(**2**) has main chain conjugation longer than that of poly(**1**). The molecular weights and photoluminescence quantum yields of the polymers obtained by the polymerization using $[(nbd)RhCl]_2$–Et_3N were larger than those of the $Rh^+(nbd)[\eta^6\text{-}C_6H_5B^-(C_6H_5)_3]$-based counterparts. The cyclic voltammograms of the polymers indicated that they had clear electrochemical properties; the onset oxidation voltage of poly(**1**) was higher than those of *N*-alkyl-substituted Cz derivatives. The polymers showed electrochromism and changed the color from pale yellow to blue by application of voltage, presumably caused by the formation of charged polaron at the Cz and TPA moieties. The temperatures for 5% weight loss of the polymers were around 350–420 °C under air, indicating the high thermal stability.

Keywords: Carbazole; Triphenylamine; Polyacetylene

---

1. Introduction

Recently, organic hole-transporting materials are intensively researched as thin layer electro-optical devices including organic light emitting diodes, solar cells, organic field-effect transistors, and photo-refractive holographic materials [1]. Among them, much attention is paid to carbazole (Cz) and triphenylamine (TPA) derivatives because they are promising candidates for photoluminescence and electroluminescence materials. Cz units are thermally stable and show photo- and electroluminescence due to the large band gap of the biphenyl unit and planarity improved by the bridging nitrogen atom [2]. TPA is a unique molecule possessing useful functions such as redox-activity, fluorescence, and ferromagnetism due to the high oxidizability of the nitrogen center, and transportability of positive charge centers via the radical cation species [3]. Meanwhile, substituted polyacetylenes exhibit unique properties such as semiconductivity, high gas permeability, helix formation, and nonlinear optical properties [4]. Introduction of Cz and TPA moieties in polyacetylene may lead to new functional materials based on the synergistic effect of Cz, TPA, and conjugated polyacetylene main chain.

Tang and coworkers have synthesized several polyacetylenes carrying Cz chromophores, which show photoluminescence and photoconductivity [5]. Tabata and coworkers have reported the synthesis and polymerization of several *N*-alkyl-3-ethynylcarbazole monomers and found that the resulting polymers take a pseudohexagonal columnar structure in the solid phase [6]. Advincula and coworkers have also

---

* Corresponding authors. Tel.: +81 75 383 2589; fax: +81 75 383 2590.
E-mail addresses: sanda@adv.polym.kyoto-u.ac.jp (F. Sanda), masuda@adv.polym.kyoto-u.ac.jp (T. Masuda).

doi:10.1016/j.polymer.2006.07.064

synthesized a series of Cz-substituted poly(phenylacetylenes) and examined the cross-linking reaction by electrochemical oxidation, where the redox potential decreases with increasing the alkyl chain length [7]. We have previously polymerized *N*-ethynylcarbazole with W, Mo, Rh, and Fe catalysts to obtain the polymer, which shows a third-order susceptibility of 18×10^{-12} esu, two orders larger than that of poly(phenylacetylene) [8]. We have also synthesized other polyacetylenes substituted with Cz, and examined the properties; e.g., poly(3,6-di-*tert*-butyl-*N*-(4-ethynylphenyl)carbazole) to find that the photoluminescence quantum yield of a W-based polymer was 15 times higher than that of an Rh-based one, and conducts electric current 40–50 times more easily under photo-irradiation than in the dark. This polymer emits electroluminescence (13–18 cd/m^2) in conjunction with iridium complexes [9].

As described above, polyacetylenes with pendant Cz are expected to show unique electronic and photonic functions. In most of these polymers, Cz is connected to the main chain through the nitrogen atom. Polyacetylenes directly connected to Cz at the benzene ring are preferable from the viewpoint of conjugation between the main chain and Cz. Cz-containing polyacetylenes are commonly poorly soluble in solvents, which makes the elucidation of their properties difficult. By introducing an appropriate substituent at the nitrogen, it is also expected to enhance the polymer solubility as well as to control the effective conjugation length and tune the properties of the resulting polymers.

On the other hand, although star-shaped, branched, and dendritic polymers of TPA have been extensively studied [10], the synthesis of TPA-containing polyacetylenes has scarcely been reported so far to our knowledge. The present study deals with the synthesis and polymerization of Cz- and TPA-based novel acetylene monomers, 3-ethynyl-9-phenylcarbazole (**1**) and *p*-(*N*,*N*-diphenylamino)phenylacetylene (**2**) (Scheme 1), and examination of the properties of the formed polymers by UV–vis spectroscopic, electrochemical, and thermogravimetric analyses.

2. Experimental section

2.1. Measurements

^{1}H (400 MHz) and ^{13}C (100 MHz) NMR spectra were recorded on a JEOL EX-400 spectrometer using tetramethylsilane (TMS) as an internal standard. IR, UV–vis, and fluorescence spectra were measured on JASCO FT/IR-4100, V-550, and FP750 spectrophotometers, respectively. Melting points (mp) were measured on a Yanaco micro melting point apparatus. Elemental analysis was carried out at the Kyoto University Elemental Analysis Center. The number- and weight-average molecular weights (M_n and M_w) of polymers were determined by gel permeation chromatography (GPC) on a JASCO GULLIVER system (PU-980, CO-965, RI-930, and UV-1570) equipped with polystyrene gel columns (Shodex columns K804, K805, and J806) using tetrahydrofuran (THF) as an eluent at a flow rate of 1.0 mL/min, calibrated by polystyrene standards at 40 °C. Thermal gravimetric analysis (TGA) was carried out with a Perkin–Elmer TGA-7. Cyclic voltammograms were measured on an HCH Instruments electro chemical analyzer ALS600A-n. The measurements were carried out with a modified ITO substrate as the working electrode coupled with a Pt plate counter and Ag/AgCl reference electrode, with a solution of a polymer (1 mM) and tetrabutylammonium perchlorate (TBAP, 0.1 M) in CH_2Cl_2. UV–vis spectra of polymer films under application of voltage were measured as follows. A polymer solution (0.2 M in $CHCl_3$) was spin coated on an ITO electrode at a spin rate of 1000 rpm, and the electrode was dried under vacuum at 50 °C for 16 h. It was immersed in a solution of TBAP (0.2 M) in acetonitrile in a quartz cell. UV–vis absorption spectra of the cell were recorded under application of voltage from 0 to 2500 mV with respect to an Ag/AgCl (saturated) reference electrode. The scans of voltage were done anodically, and 5-min equilibration time was taken before each spectral scan to minimize the transient effect. The applied voltages reported herein were calibrated using ferrocene as a standard.

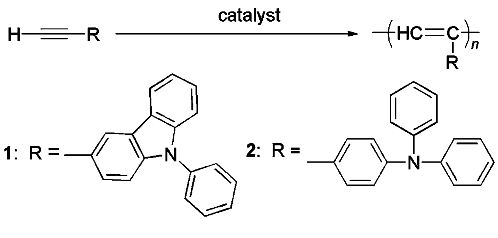

Scheme 1. Polymerization of **1** and **2**.

2.2. Materials

Unless otherwise stated, reagents were purchased and used without purification. 3-Iodo-9-phenylcarbazole [11] and *N*,*N*-diphenyl-4-bromoaniline [12] were synthesized according to the literature. Solvents for polymerization were purified before use by the standard methods.

2.3. Synthesis of 3-ethynyl-9-phenylcarbazole (*1*)

A 300 mL three-necked flask was equipped with a three-way stopcock and a magnetic stirring bar, and flushed with dry nitrogen. 3-Iodo-9-phenylcarbazole (4.3 g, 12 mmol), (trimethylsilyl)acetylene (2.1 mL, 14 mmol), bis(triphenylphosphine)palladium dichloride (82 mg, 0.12 mmol), triphenylphosphine (92 mg, 0.35 mmol), cuprous iodide (89 mg, 0.47 mmol), triethylamine (100 mL), and piperidine (20 mL) were fed into the flask. The mixture was stirred at room temperature overnight. After that, triethylamine and piperidine were evaporated off, and diethyl ether (80 mL) was added to the residue. Insoluble salt was filtered off, and the filtrate was washed with 1 N hydrochloric acid and then with water. The ethereal solution was dried over anhydrous Na_2SO_4, and concentrated with a rotary evaporator. Purification of the crude product by flash silica gel column chromatography eluted with *n*-hexane/ethyl acetate = 4/1 (volume ratio) provided a yellow

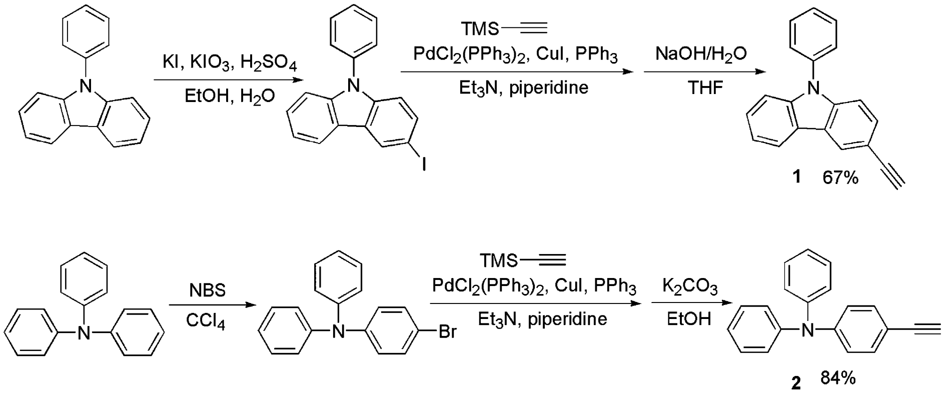

Scheme 2. Synthetic routes of **1** and **2**.

Table 1
Polymerization of **1**[a]

Run	Catalyst	Cocatalyst	Solvent	Yield[b] (%)	M_n[c]	M_w/M_n[c]	Color
1	$[(nbd)RhCl]_2$	Et_3N	Toluene	83	100 000	2.43	Orange
2	$[(nbd)RhCl]_2$	Et_3N	$CHCl_3$	84	27 900	2.28	Orange
3	$[(nbd)RhCl]_2$	Et_3N	CH_2Cl_2	88	81 300	1.77	Orange
4	$[(nbd)RhCl]_2$	Et_3N	o-$Cl_2C_6H_4$	99	69 800	3.17	Orange
5	$[(nbd)RhCl]_2$	Et_3N	Anisole	77	52 700	2.54	Orange
6	$[(nbd)RhCl]_2$	Et_3N	THF	90	36 000	2.33	Orange
7	$[(nbd)RhCl]_2$	Et_3N	MeOH	36	7600	4.33	Orange
8	$[(nbd)RhCl]_2$	n-BuLi[d]	Toluene	96	80 800	3.18	Orange
9	$[(nbd)RhCl]_2$	$KN(SiMe_3)_2$[e]	Toluene	95	18 800	3.54	Orange
10	$Rh^+(nbd)[\eta^6\text{-}C_6H_5B^-(C_6H_5)_3]$	None	Toluene	95	15 500	1.95	Orange
11	WCl_6	Ph_4Sn[f]	Toluene	32	2700	1.86	Pale yellow
12	$MoCl_5$	n-Bu_4Sn[g]	Toluene	0	–	–	–

[a] $[M]_0 = 0.20$ M, [Rh] = 2.0 mM, $[Et_3N] = 10$ mM, 30 °C, 24 h.
[b] Acetone-insoluble part.
[c] Determined by GPC eluted with THF, polystyrene calibration.
[d] [n-BuLi] = 2.0 mM.
[e] [Rh]/[K] = 1.0.
[f] $[MoCl_5]/[n\text{-}Bu_4Sn] = 0.50$.
[g] $[WCl_6]/[Ph_4Sn] = 0.50$.

Table 2
Polymerization of **2**[a]

Run	Catalyst	Cocatalyst	Solvent	Yield[b] (%)	M_n[c]	M_w/M_n[c]	Color
1	$[(nbd)RhCl]_2$	Et_3N	Toluene	82	99 000	3.56	Red
2	$[(nbd)RhCl]_2$	Et_3N	$CHCl_3$	84	974 000	3.87	Red
3	$[(nbd)RhCl]_2$	Et_3N	CH_2Cl_2	90	588 000	4.10	Red
4	$[(nbd)RhCl]_2$	Et_3N	o-$Cl_2C_6H_4$	94	586 000	3.56	Red
5	$[(nbd)RhCl]_2$	Et_3N	Anisole	95	101 000	8.58	Red
6	$[(nbd)RhCl]_2$	Et_3N	THF	85	29 900	2.24	Red
7	$[(nbd)RhCl]_2$	Et_3N	MeOH	20	98 000	18.1	Red
8	$[(nbd)RhCl]_2$	n-BuLi[d]	Toluene	96	31 000	11.5	Red
9	$[(nbd)RhCl]_2$	$KN(SiMe_3)_2$[e]	Toluene	97	13 900	12.9	Red
10	$Rh^+(nbd)[\eta^6\text{-}C_6H_5B^-(C_6H_5)_3]$	None	Toluene	87	31 800	2.95	Red
11	WCl_6	Ph_4Sn[f]	Toluene	37	3200	1.37	Pale yellow
12	$MoCl_5$	n-Bu_4Sn[g]	Toluene	3	1500	1.59	Pale yellow

[a] $[M]_0 = 0.20$ M, [Rh] = 2.0 mM, $[Et_3N] = 10$ mM, 30 °C, 24 h.
[b] Acetone-insoluble part.
[c] Determined by GPC eluted with THF, polystyrene calibration.
[d] [n-BuLi] = 2.0 mM.
[e] [Rh]/[K] = 1.0.
[f] $[MoCl_5]/[n\text{-}Bu_4Sn] = 0.50$.
[g] $[WCl_6]/[Ph_4Sn] = 0.50$.

liquid (yield 2.88 g, 67%). THF (80 mL) and aqueous 0.5 M NaOH (100 mL) were added to the liquid, and the resulting mixture was stirred at room temperature overnight. The mixture was concentrated, and ether was added to the residue. The ether solution was washed subsequently with 1 N HCl and water. The organic layer was dried over anhydrous Na_2SO_4 and concentrated to afford a yellow liquid. It was purified by silica gel column chromatography eluted with *n*-hexane/ethyl acetate 4/1 (volume ratio) and further purified by preparative HPLC eluted with chloroform to yield pale yellow liquid. Yield 2.10 g (75%). IR (KBr): 3432, 3290, 3061, 2102, 1625, 1597, 1500, 1456, 1231, 842, 810, 760, 699 cm^{-1}. ^1H NMR (400 MHz, δ in ppm, $CDCl_3$): 3.00 (1H, $\equiv$CH), 7.17–8.24 (10H, Ar). ^{13}C NMR (100 MHz, δ in ppm, $CDCl_3$): 75.4 ($\equiv$CH), 84.81 ($-C\equiv$CH), 109.97, 113.14, 113.18, 120.42, 122.70, 123.28, 124.36, 124.57, 126.48, 127.05, 127.78, 129.67, 129.87, 129.95, 137.14, 141.31. Anal. Calcd for $C_{20}H_{13}N$: C, 89.86; H, 4.90; N, 5.24. Found: C, 89.60; H, 4.90; N, 5.16.

2.4. Synthesis of p-(N,N-diphenylamino)phenylacetylene (2)

The compound was synthesized from *N,N*-diphenyl-4-bromoaniline in a manner similar to **1**. Yield 85%. Mp: 104–105 °C. IR (KBr): 3450, 3265, 3058, 3034, 2102, 1599, 1450, 1318, 1174, 830, 755, 665 cm^{-1}. ^1H NMR (400 MHz, in ppm, $CDCl_3$): 3.00 (s, 1H, $\equiv$CH), 6.93 (m, 2H), 7.05 (m, 6H, Ar), 7.31 (m, 6H, Ar). ^{13}C NMR ($CDCl_3$): 76.17 ($\equiv$CH), 83.89 ($-C\equiv$CH), 148.3, 147.09, 133.02, 129.38, 125.00, 123.61, 122.02, 114.73. Anal. Calcd for $C_{20}H_{15}N$: C, 89.19; H, 5.61; N, 5.20. Found: C, 89.05; H, 5.86; N, 5.09.

2.5. Polymerization

All the polymerizations were carried out in a Schlenk tube equipped with a three-way stopcock under dry nitrogen. The polymerization mixture was poured into a large amount of acetone to precipitate a polymer. It was separated from the supernatant by filtration and dried under reduced pressure.

2.6. Spectroscopic data of the polymers

Poly(**1**): ^1H NMR (400 MHz, in ppm, $CDCl_3$): 6.0–8.2 (broad m). IR (KBr): 3450, 3041, 1596, 1500, 1452, 1230, 802, 758, 743, 700 cm^{-1}. Poly(**2**): ^1H NMR (400 MHz, in ppm, $CDCl_3$): 5.8–7.9 (broad m). IR (KBr): 3415, 3060, 3030, 1588, 1489, 1267, 1176, 1070, 1026, 897, 748, 692 cm^{-1}.

3. Results and discussion

3.1. Monomer synthesis

Scheme 2 illustrates the synthetic routes for Cz- and TPA-containing monomers **1** and **2**. They were synthesized by the Sonogashira coupling reaction of 3-iodo-9-phenylcarbazole and *N,N*-diphenyl-4-bromoaniline with trimethysilylacetylene, followed by desilylation using aqueous NaOH and K_2CO_3 in 67 and 84% yields, respectively. The structure of the monomers were confirmed by IR, ^1H, and ^{13}C NMR spectra besides elemental analysis.

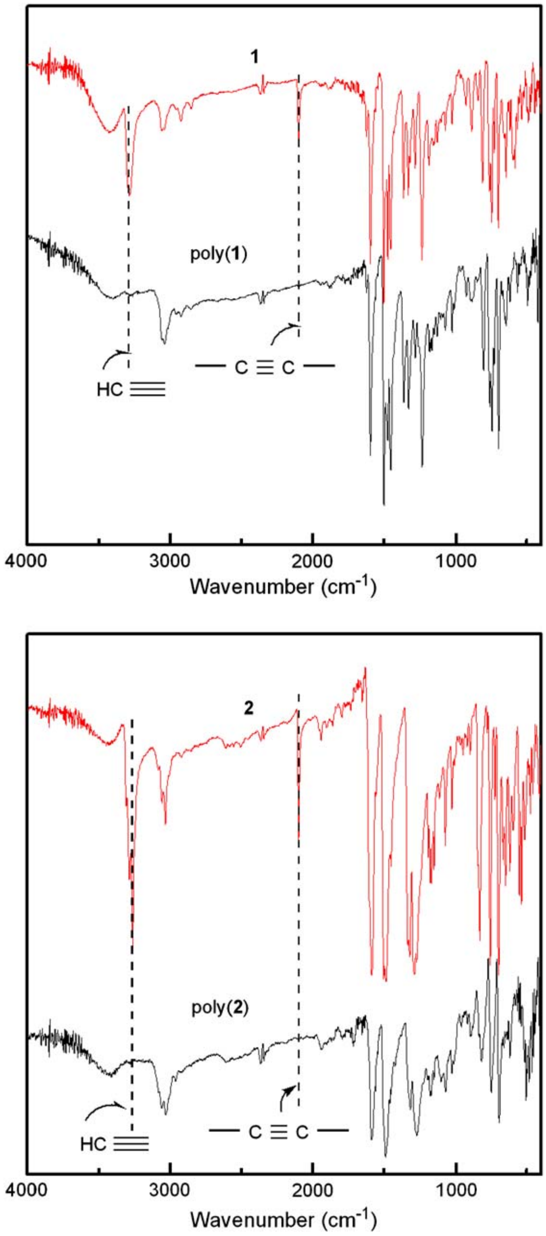

Fig. 1. IR spectra of **1**, poly(**1**), **2**, and poly(**2**). Polymer samples from run 1 in Table 1 and run 1 in Table 2.

3.2. Polymerization

Table 1 summarizes the conditions and results of the polymerization of Cz-containing monomer **1** catalyzed with $[(nbd)RhCl]_2$, $Rh^+(nbd)[\eta^6\text{-}C_6H_5B^-(C_6H_5)_3]$, WCl_6, and $MoCl_5$ in toluene, $CHCl_3$, CH_2Cl_2, *o*-$Cl_2C_6H_4$, anisole, THF, and methanol at 30 °C for 24 h. When $[(nbd)RhCl]_2$–Et_3N was used (Table 1, runs 1–7), the polymerization mixture became orange within 3 min, and gradually turned dark orange with increasing viscosity. Pouring the reaction mixture into a large amount of acetone precipitated a fine orange powdery

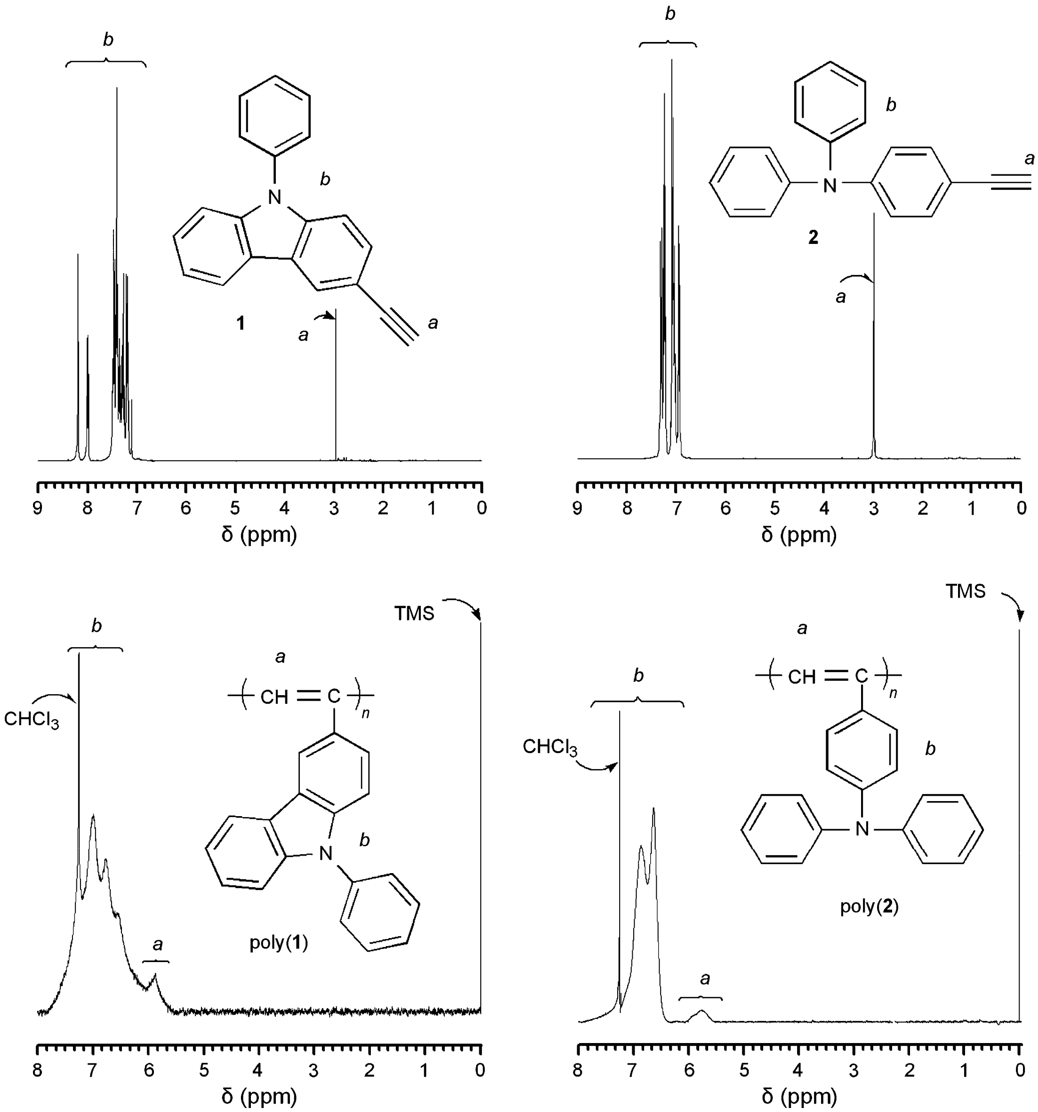

Fig. 2. ^{1}H NMR spectra of **1**, poly(**1**), **2**, and poly(**2**). Polymer samples from run 1 in Table 1 and run 1 in Table 2.

polymer with moderate molecular weights in good yields, except the case when MeOH was used as the solvent (Table 1, run 7). In MeOH, it seems that the incomplete solubility of the monomer and polymer caused this unsatisfactory result. Toluene (Table 1, run 1) was the most effective to obtain the polymer with a high M_n among the solvents used. $[(nbd)RhCl]_2$–Et_3N gave the polymer with an M_n higher than $Rh^+(nbd)[\eta^6\text{-}C_6H_5B^-(C_6H_5)_3]$ did in toluene (Table 1, runs 1 and 10). When n-BuLi and $KN(SiMe_3)_2$ were used as cocatalysts (Table 1, runs 8 and 9) in toluene, the reaction mixture increased the viscosity quickly to become solid in 3 h. However, the M_n of the formed polymer was lower, and the polydispersity was larger than the case of Et_3N as a cocatalyst, wherein the polymerization mixture was homogeneous till the final stage. The yield and M_n of the polymer obtained by WCl_6-catalyzed polymerization were very low (Table 1, run 11), and no polymer was obtained with $MoCl_5$ (Table 1, run 12). In our previous paper, Rh catalysts also afforded a polymer of a phenylacetylene monomer containing Cz in a higher yield than W catalyst did [13]. Rh and W catalysts commonly give *cis*- and *trans*-rich substituted polyacetylenes, respectively, and the latter is sterically unfavorable than the former. In the present case, it is likely that the bulky Cz moieties resulted in the low yield and M_n of the polymer obtained by the W-based polymerization.

Table 2 summarizes the conditions and results of the polymerization of TPA-containing monomer **2**. The color of the formed polymers was dark-red, and the molecular weights were larger than the ones obtained from **1**. High-molecular-weight polymers were obtained especially by the polymerization with $[(nbd)RhCl]_2$–Et_3N in $CHCl_3$, CH_2Cl_2 and o-$Cl_2C_6H_4$ (Table 2, runs 2–4). The solvents affected the polymerization of **2** largely than that of **1**. The results of the polymerization of **1** and **2** clearly indicate that the combination of $[(nbd)RhCl]_2$ with Et_3N is the best choice of catalyst to obtain the polymers with high molecular weights in good yields.

Both poly(**1**) and poly(**2**) were soluble in toluene, $CHCl_3$, CH_2Cl_2, o-$Cl_2C_6H_4$, anisole, and THF, but insoluble in MeOH, benzene, hexane, and acetone, irrespective of the catalyst used in the polymerization. The solubility of poly(**1**) was apparently good compared to that of poly(*N*-ethynylcarbazole) [8] and poly[*N*-(4-ethynylphenyl)carbazole] reported previously [14]; the latter two polymers obtained with [(nbd)RhCl]$_2$–Et$_3$N catalyst are insoluble in common organic solvents including toluene, CHCl$_3$ and THF. Thus, it is clear that the substitution position greatly affects the solubility of the polymers.

3.3. Polymer structure

The polymer structures were examined by ^{1}H NMR and IR spectroscopies as shown in Figs. 1 and 2. The IR spectra of the polymers obtained by the polymerization with [(nbd)RhCl]$_2$–Et$_3$N, Rh$^+$(nbd)[η^6-C$_6$H$_5$B$^-$(C$_6$H$_5$)$_3$], and W catalysts exhibited almost the same patterns. No absorption peaks around 3300 and 2102 cm^{-1} attributable to the stretching vibration of ≡C–H and C≡C bonds were observed in the IR spectra of the polymers. In the ^{1}H NMR spectra of the polymers, no signal around 3.0 ppm assignable to acetylenic proton of the monomers was observed. All these results clearly indicate that the acetylene polymerization took place to form the polymers composed of alternating single and double bonds. It has been reported that Rh catalysts predominantly afford polyacetylenes with *cis* structure, while W catalysts afford *trans*-rich polyacetylenes [4]. In the present study, the ^{1}H NMR signals of the polymers appeared very broadly, and the signal assignable to the olefinic proton of the polyacetylene main chain coalesced with aromatic proton signals, which made it impossible to determine the *cis*/*trans* ratio of the main chain. We also measured the ^{13}C NMR spectra of the polymers in addition to the IR and ^{1}H NMR spectra, but the ^{13}C NMR signals were very broad, and gave no useful information on the polymer structure.

3.4. Polymer properties

Fig. 3 depicts the UV–vis spectra of poly(**1**) and poly(**2**) obtained by the polymerization using Rh catalysts, along with the monomers, 9-PhCz, and TPA for comparison. The spectrum of **1** was consistent with that of 9-PhCz showing the absorption peaks at 295, 335, and 350 nm attributable to Cz, and the absorption band tailed from 280 to 300 nm. Both of the polymers exhibited absorption peaks at longer wavelength than the corresponding monomers did regardless of using [(nbd)RhCl]$_2$ and Rh$^+$(nbd)[η^6-C$_6$H$_5$B$^-$(C$_6$H$_5$)$_3$], which should result from the conjugation of the polyacetylene main chain. The absorption spectra of poly(**1**) were consistent with the fact that Cz moieties incorporated into polyacetylene as pendant groups. The absorption band in the range 370–550 nm is due to the π–π* absorption of the polyacetylene main chain. The other peaks below 350 nm are attributed to the absorption by the π–π*, *n*–π*, and benzenoid transitions of carbazolyl and phenyl groups. The absorption band edge of Rh-based poly(**1**) was 550 nm, 20–40 nm longer than those of Rh-based poly(3,6-di-*tert*-butyl-*N*-(4-ethynylphenyl)carbazole) [9] previously reported. We can say that the conjugation length of poly(**1**) is longer than that of poly(3,6-di-*tert*-butyl-*N*-(4-ethynylphenyl)carbazole) as expected. Unfortunately, we cannot compare the UV–vis spectrum of poly(**1**) with those of Rh-based poly(*N*-ethynylcarbazole) [8] and poly(*N*-(4-ethynylphenyl)carbazole) [14], because the latter two polymers are solvent insoluble. Poly(**2**) exhibited the UV–vis absorption peaks derived from the TPA moieties at 250–350 nm, and polyacetylene backbone above 350 nm. The UV–vis absorption band edge of poly(**2**) was positioned at a longer wavelength (600 nm) than that of poly(**1**) (550 nm), which indicates the former polymer has a main chain conjugation longer than that of the latter.

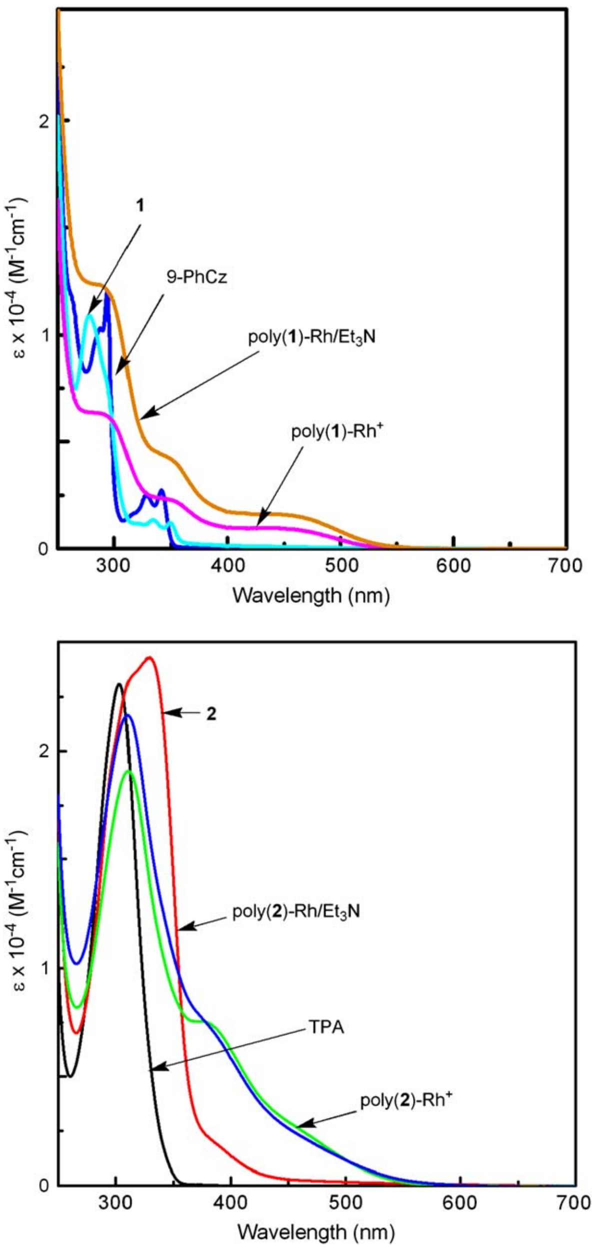

Fig. 3. UV–vis spectra of **1**, poly(**1**) and **2**, poly(**2**) measured in CHCl$_3$, along with 9-PhCz and TPA. Concentrations; **1**: 1.86×10^{-5} M, poly(**1**)-Rh/Et$_3$N: run 1 in Table 1, 1.75×10^{-5} M, poly(**1**)-Rh$^+$: run 10 in Table 1, 1.03×10^{-5} M, **2**: 3.85×10^{-5} M, poly(**2**)-Rh/Et$_3$N: run 1 in Table 2, 4.94×10^{-5} M, poly(**2**)-Rh$^+$: run 10 in Table 2, 1.69×10^{-5} M, 9-PhCz: 2.33×10^{-5} M, TPA: 9.17×10^{-5} M.

Fig. 4 shows the fluorescence spectra of poly(**1**) and poly(**2**) obtained by the polymerization using Rh catalysts, along with those of the monomers, 9-PhCz, and TPA. The polymer solution emitted luminescence, whose maximum wavelength was observed at 390 nm upon excitation at 294 nm for poly(**1**), and at 410 nm upon excitation at 310 nm for poly(**2**). It is noteworthy that the fluorescence quantum yields of the $[(nbd)RhCl]_2$–Et_3N-based polymers were larger than those of $Rh^+(nbd)[\eta^6\text{-}C_6H_5B^-(C_6H_5)_3]$-based counterparts, and smaller than that of the corresponding monomers. Poly(**1**) showed luminescence at a wavelength ca. 10 nm longer than that of **1**, while poly(**2**) did at a wavelength 100 nm longer than that of **2**. It was also found that the fluorescence quantum yields of the monomers were larger than those of 9-PhCz and TPA.

Fig. 5 depicts the cyclic voltammetric (CV) curves of poly(**1**) and poly(**2**). The oxidation of poly(**1**) initiated at 1.10 V on the first cycle was somewhat higher than those of *N*-alkyl-substituted Cz derivatives reported so far (0.7–0.8 V) [15]. *N*-Phenyl group may cause this result due to the steric hindrance and/or electronic factors. As the CV scans continued, poly(**1**) showed one oxidation peak at 1.30 V, and two reduction peaks at 0.70 and 1.50 V, which were absent in the first cycle. It seems that a conducting polymer film was formed on the working electrode surface, and the film thickness gradually increased upon CV scanning. The potential shift of this maximum provided the information about the increase of the electrical resistance in the polymer film; over-potential was needed to overcome the resistance. On the other hand,

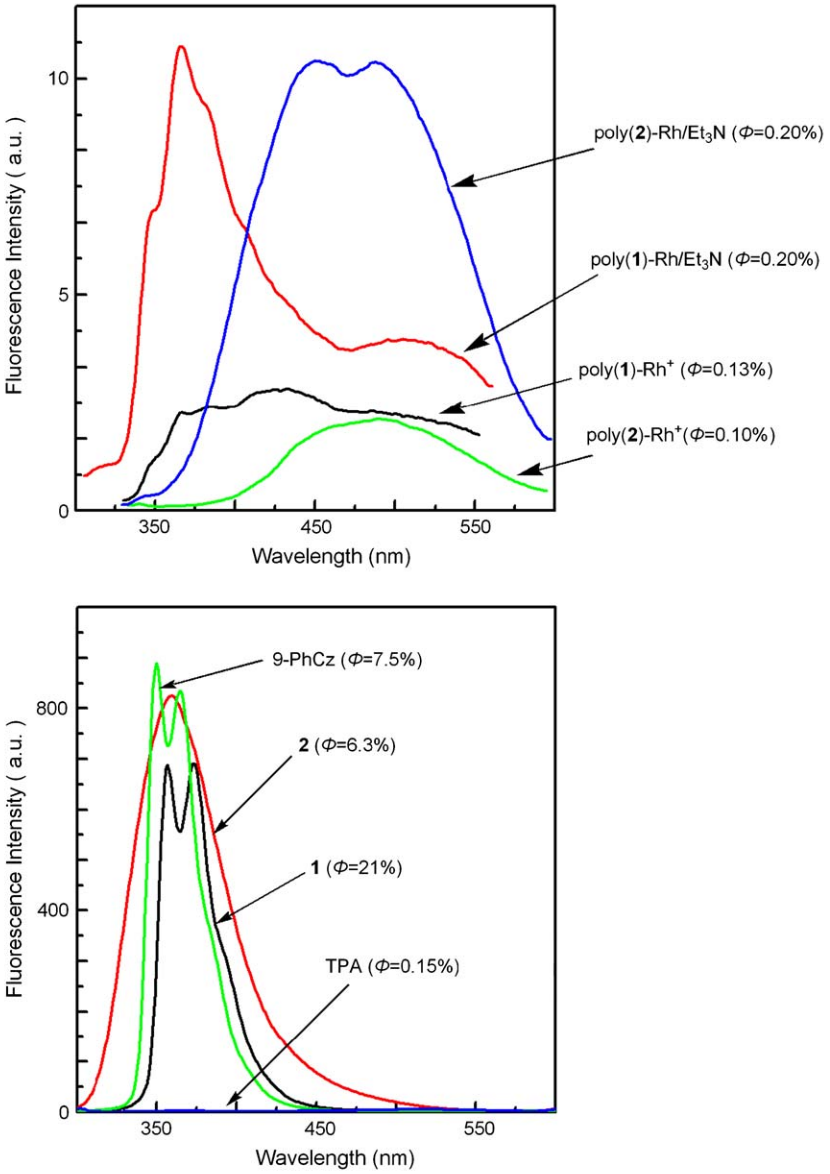

Fig. 4. Fluorescence spectra of **1**, poly(**1**), **2**, and poly(**2**) measured in $CHCl_3$, along with 9-PhCz and TPA. Concentrations and excited wavelength; **1**: 1.86×10^{-5} M, 278 nm, poly(**1**)-Rh/Et_3N: run 1 in Table 1, 1.75×10^{-5} M, 294 nm, poly(**1**)-Rh^+: run 10 in Table 1, 1.03×10^{-5} M, 294 nm, **2**: 3.85×10^{-5} M, 329 nm, poly(**2**)-Rh/Et_3N: run 1 in Table 2, 4.94×10^{-5} M, 310 nm, poly(**2**)-Rh^+: run 10 in Table 2, 1.69×10^{-5} M, 310 nm, 9-PhCz: 2.33×10^{-5} M, 294 nm, TPA: 9.17×10^{-5} M, 303 nm. The intensities are normalized based on the concentrations of Cz unit.

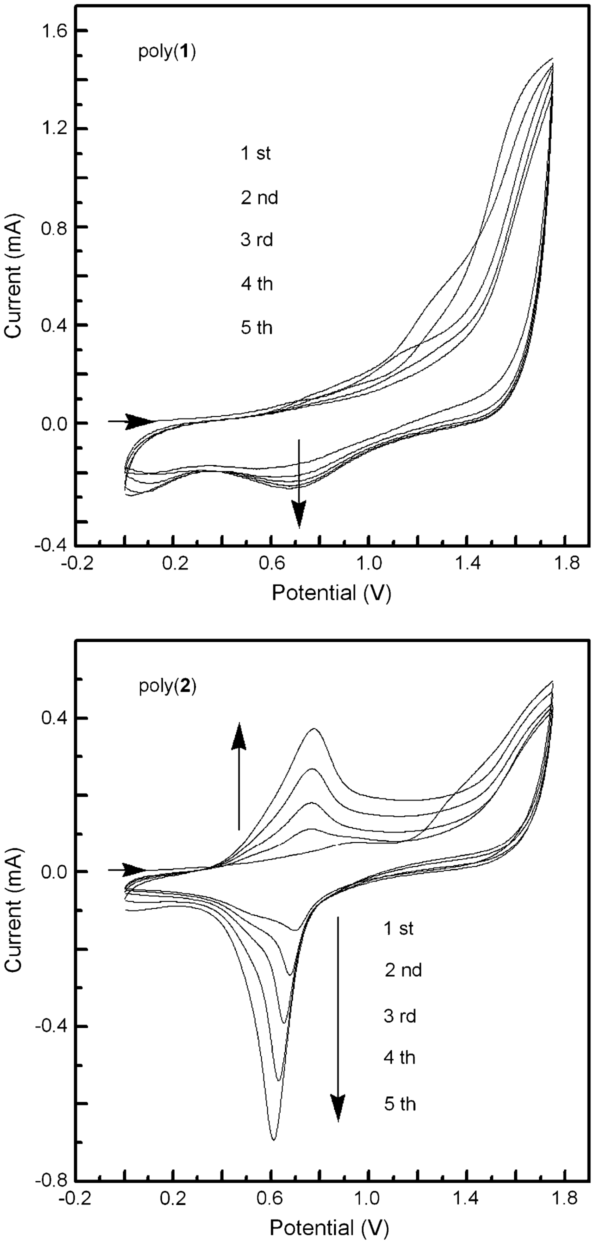

Fig. 5. Cyclic voltammograms of poly(**1**) and poly(**2**) measured at a scan rate of 0.1 V/s, vs Ag/Ag$^+$ in a TBAP solution. Poly(**1**): run 1 in Table 1, poly(**2**): run 1 in Table 2.

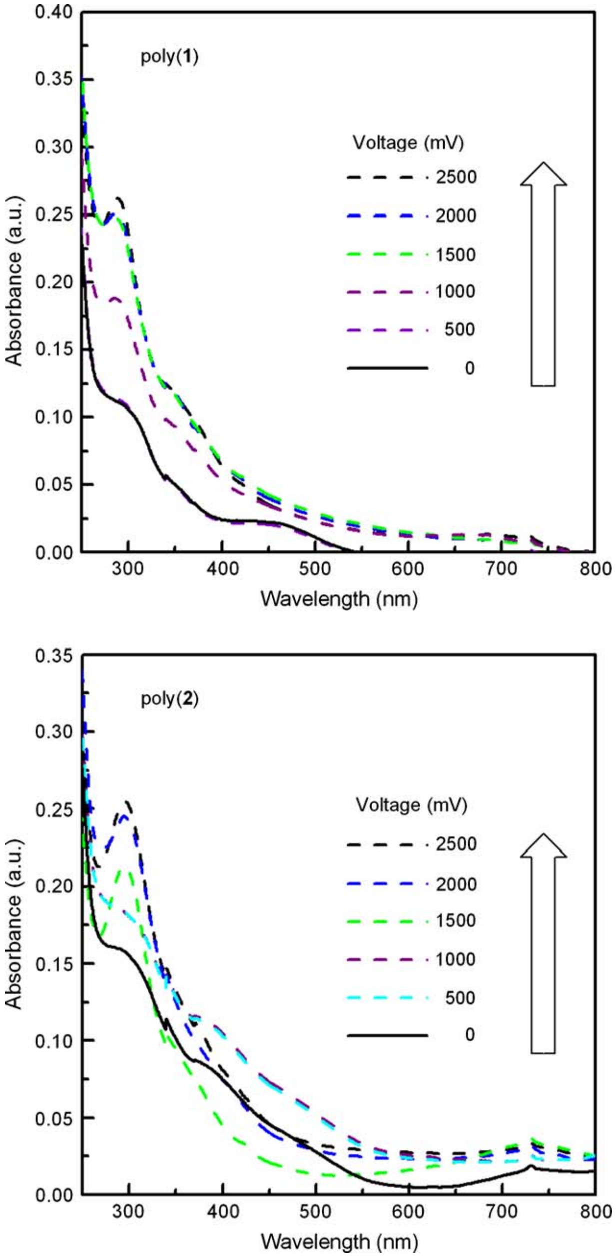

Fig. 6. UV–vis spectra of poly(**1**) and poly(**2**) films under application of voltage. Poly(**1**): run 1 in Table 1, poly(**2**): run 1 in Table 2.

the oxidation of poly(**2**) was initiated at 0.45 V in the first scan, which was lower than that of TPA showing a stepwise-oxidation wave at 1.25 V [16]. Poly(**2**) showed an oxidation peak at 0.80 V and the corresponding reduction peak at 0.65 V. The oxidation and reduction potentials of poly(**2**) gradually shifted to positive and negative fields, respectively.

Fig. 6 depicts the UV–vis spectra of voltage-applied films fabricated by spin coating of poly(**1**) and poly(**2**) solutions. Before electric potential was applied, the pale yellowish polymeric film of poly(**1**) showed an intense absorption at 294 nm, which was the same as the polymer solution. By setting the potential to 1500 mV, the film turned into blue to give an intensive absorption band at 294 nm. At raising the voltage, the absorption at 294 nm became large accompanying the increase of absorption around 700 nm, attributable to the formation of charged polaron at the Cz moiety [15]. Further increase of the applied potential to 2500 mV resulted in the color change of the film into deep blue. A similar change based on charged polaron-formation was observed also in the case of poly(**2**); the intensities of absorption peak at 303 nm and around 700 nm increased by application of voltage [17]. Poly(**2**) apparently turned the color around 1000 mV, lower than that of poly(**1**). This agrees with the fact that poly(**2**) is more easily oxidizable than is poly(**1**) as confirmed by CV (see Fig. 5).

Fig. 7 depicts the TGA traces of the polymers obtained by the polymerization with Rh catalysts. The temperatures for 5% weight loss were around 350–420 °C under air, which

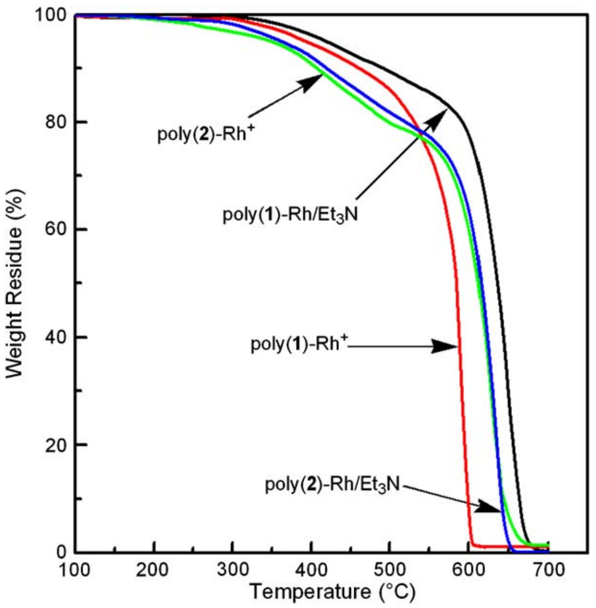

Fig. 7. TGA curves of poly(**1**) and poly(**2**) measured at a heating rate of 10 °C/min in air. poly(**1**)-Rh/Et_3N: run 1 in Table 1, poly(**1**)-Rh^+: run 10 in Table 1, poly(**2**)-Rh/Et_3N: run 1 in Table 2, poly(**2**)-Rh^+: run 10 in Table 2.

were much higher than that of poly(phenylacetylene) [18]. The present polymers thermally degraded more slowly than poly(phenylacetylene), which may be attributable to the bulky Cz and TPA side chains. They completely lost their weights around 700 °C. The $[(nbd)RhCl]_2$–Et_3N-based polymers were more stable than the $Rh^+(nbd)[\eta^6\text{-}C_6H_5B^-(C_6H_5)_3]$-based counterparts, presumably due to the difference in molecular weights. Poly(**1**) was more stable than poly(**2**). The rigid structure of Cz moieties may be favorable to enhance the thermal stability than TPA.

4. Conclusions

In this article, we have demonstrated the synthesis of novel Cz and TPA-containing conjugated polymers, poly(3-ethynyl-9-phenylcarbazole) [poly(**1**)] and poly[*p*-(*N*,*N*-diphenylamino)-phenylacetylene] [poly(**2**)], and examined their properties by UV–vis spectroscopic, electrochemical, and thermogravimetric analyses. It was found that the polymers exhibited UV–vis absorption peaks derived from the Cz and TPA moieties at 250–350 nm and polyacetylene backbone above 350 nm. The UV–vis absorption band edge wavelengths of the polymers were longer than those of the corresponding monomers. Poly(**2**) exhibited a UV–vis absorption peak at a longer wavelength than poly(**1**) did, which indicates that poly(**2**) has a main chain conjugation longer than that of poly(**1**). The molecular weights and photoluminescence quantum yields of the polymers obtained by the polymerization using $[(nbd)RhCl]_2$–Et_3N were higher than those of the $Rh^+(nbd)[\eta^6\text{-}C_6H_5B^-(C_6H_5)_3]$-based counterparts. The polymers indicated clear electrochemical properties, which were confirmed by CV measurement. The polymers showed electrochromism; i.e., they changed the color from pale yellow to blue by application of voltage, presumably caused by the formation of charged polaron at the Cz and TPA moieties. These polymers were thermally stable; the temperatures for 5% weight loss were around 350–420 °C under air.

Acknowledgments

This research was partly supported by a Grant-in-Aid for Science Research in a Priority Area "Super-Hierarchical Structures (No. 446)" from the Ministry of Education, Culture, Sports, Science and Technology, Japan.

References

[1] (a) Burroughs H, Bradley DDC, Brown AR, Marks RN, Mackay K, Friend RH, et al. Nature 1990;347:539;
(b) Kraft A, Grimsdale AC, Holmes AB. Angew Chem Int Ed 1998;37:402;
(c) Friend RH, Gymer RW, Holmes AB, Burroughes JH, Marks RN, Taliani C, et al. Nature 1999;397:121;
(d) Bach U, Lupo D, Compte P, Moser JE, Weissertel F, Salbeck J, et al. Nature 1998;395:583.

[2] (a) Wang YZ, Epstein AJ. Acc Chem Res 1999;32:217;
(b) Grazulevicius JV, Strohriegl P, Pielichowski J, Pielichowski K. Prog Polym Sci 2003;28:1297.

[3] (a) Bernius MT, Inbasekaran M, O'Brien J, Wu WS. Adv Mater 2000;12:1737;
(b) Shirota Y. J Mater Chem 2000;10:1;
(c) Thelakkat M. Macromol Mater Eng 2002;287:442.

[4] (a) Jack W, Lam Y, Tang BZ. Acc Chem Res 2005;38:745;
(b) Nagai K, Masuda T, Nakagawa T, Freeman BD, Pinnau I. Prog Polym Sci 2001;26:721;
(c) Masuda T. Acetylenic polymers. In: Salamone JC, editor. Polymeric material encyclopedia, vol. 1. New York: CRC; 1996. p. 32.

[5] (a) Tang BZ, Chen HZ, Xu RS, Lam JWY, Cheuk KKL, Wong HNC, et al. Chem Mater 2000;12:213;
(b) Pui-Sze Lee P, Geng Y, Kwok HS, Tang BZ. Thin Solid Films 2000;363:149.

[6] Tabata M, Fukushima T, Sadahiro Y. Macromolecules 2004;37:4342.

[7] (a) Onishi K, Advincula RC, Abdul Karim SM, Nakai T, Masuda T. ACS Polym Prepr 2002;43(1):171;
(b) Nakano M, Masuda T, Higashimura T. Polym Bull 1995;34:191.

[8] Sata T, Nomura R, Wada T, Sasabe H, Masuda T. J Polym Sci Part A Polym Chem 1998;36:2489.

[9] Sanda F, Nakai T, Kobayashi N, Masuda T. Macromolecules 2004;37:2703.

[10] Cho JS, Kimoto A, Higuchi M, Yamamoto K. Macromol Chem Phys 2005;206:635.

[11] Maria E, Sergio MB, Rosa EB. J Heterocycl Chem 2002;39:933.

[12] Bacher E, Bayerl M, Rudati P, Reckefuss N, Müller CD, Meerholz K, et al. Macromolecules 2005;38:1640.

[13] Sanda F, Kawasaki R, Shiotsuki M, Masuda T. Polymer 2004;45:7831.

[14] Sanda F, Kawaguchi T, Masuda T. Macromolecules 2003;36:2224.

[15] Wei ZH, Xu JK, Nie GM, Du YK, Pu SZ. J Electroanal Chem 2006;589:112.

[16] Chiu KY, Su TX, Li JH, Lin TH, Liou GS, Cheng SH. J Electroanal Chem 2005;575:95.

[17] Chou MY, Leung MK, Su YO, Chiang CL, Lin CC, Liu JH, et al. Chem Mater 2004;16:654.

[18] Nakai T, Karim SMA, Teraguchi M, Sanda F, Masuda T. J Macromol Sci Pure Appl Chem 2002;A39:935.